View metadata, citation and similar papers at core.ac.uk

brought to you by CORE

provided by University of Queensland eSpace

PROCEEDINGS OF SPIE

SPIEDigitalLibrary.org/conference-proceedings-of-spie

Optical properties of covalently anchored single-walled carbon nanotube arrays on silicon (100) surfaces

Jingxian Yu, Joe Shapter, Jamie Quinton, Martin Johnston, David Beattie

Jingxian Yu, Joe Shapter, Jamie Quinton, Martin Johnston, David Beattie, "Optical properties of covalently anchored single-walled carbon nanotube arrays on silicon (100) surfaces," Proc. SPIE 6415, Micro- and Nanotechnology: Materials, Processes, Packaging, and Systems III, 641504 (20 December 2006); doi: 10.1117/12.695611

SPIE.

Event: SPIE Smart Materials, Nano- and Micro-Smart Systems, 2006, Adelaide, Australia

Downloaded From: https://www.spiedigitallibrary.org/conference-proceedings-of-spie on 4/26/2018 Terms of Use: https://www.spiedigitallibrary.org/terms-of-use

Optical properties of covalently anchored single-walled carbon nanotube arrays on silicon (100) surfaces

Jingxian Yu[a], Joe Shapter[*, a], Jamie Quinton[a], Martin Johnston[a] and David Beattie[b]
[a]School of Chemistry, Physics and Earth Sciences, Flinders University, SA 5042, Australia
[b] Ian Wark Research Institute, University of South Australia, SA 5095, Australia

ABSTRACT

In this paper a new approach for directly organizing single-walled carbon nanotubes (SWCNTs) onto a silicon (100) surface by the surface condensation reaction with hydroxyl terminated silicon is presented. X-ray photoelectron spectra, Raman spectroscopy and atomic force microscopy show that the shortened SWCNTs have been organized successfully on silicon. The optical properties of SWCNT array exhibit strong fluorescence in the visible wavelength range from 650-800 nm. The fluorescence can be attributed to the coupling effects between attached SWCNTs and silicon substrate.

Keywords: single-walled carbon nanotubes, silicon, atomic force microscopy, Raman, fluorescence

1. INTRODUCTION

Single-walled carbon nanotubes (SWCNTs) are elongated members of the fullerene family. These one-dimensional molecular structures have recently become the focus of intense multidisciplinary study due to their unique structure, chirality-dependent conductivity, high mechanical strength and good chemical stability. These properties make carbon nanotubes excellent candidates for electron field emission sources, scanning probe tips, nanoelectronic devices, energy storage devices, actuators, as well as building blocks for chemical and biochemical sensors. However, most of these potential applications require surface-mounted aligned carbon nanotube arrays grown with large-scale control of location and orientation. In this regard, many efforts have been undertaken to fabricate highly oriented carbon nanotubes on device surfaces based on direct growth by chemical vapor deposition and self-assembling techniques[1, 2].

The direct patterned growth of aligned carbon nanotube arrays has been widely explored and successfully developed using chemical vapour deposition techniques. However, these methods have limitations with regard to large-scale applications because of the high growth temperature required, poor adhesion between nanotubes and substrates, success only for multi-walled carbon nanotubes and the closed ends of carbon nanotubes [2-4]. Clearly, the high growth temperature makes positioning carbon nanotubes onto temperature sensitive substrates such as integrated circuit (ICs) impossible. In addition, poor adhesion results in long term reliability issues and high contact resistances. In addition, due to the capped ends of the nanotubes, further chemical modification will be difficult because continued processing of surface-mounted nanotubes may have a detrimental effect on the substrate itself.

Several methods have been developed for alkanethiol self assembled monolayer (SAM) immobilisation onto metal surfaces and these have proved to be particularly powerful for SWCNTs integration at low temperature[5]. However, their widespread technological application is uncertain due to issues related to the long-term stability of alkanethiols on gold surfaces. Dynamic studies of alkanethiols on gold surfaces have revealed several serious disadvantages in the thiol-gold chemistry. It is for these reasons that recent attention has been focussed on the covalent attachment of carbon nanotubes to surfaces. For example, Jung [6] has reported a novel method for producing high density carbon nanotube arrays through the formation of an amine terminated surface by treatment of a glass surface with an aminosiloxane followed by subsequent attachment of shortened carbon nanotubes via a condensation reaction between amine and carboxylic acid groups. These SWCNT layers have excellent surface adhesion because of their strong chemical bonding to the substrate. A disadvantage of this approach is the presence of the intervening self-assembled monolayer, which is an impediment in situations where electron transduction to the substrate is desirable.

* Email: joe.shapter@flinders.edu.au (J. Shapter)

Micro- and Nanotechnology: Materials, Processes, Packaging, and Systems III,
edited by Jung-Chih Chiao, Andrew S. Dzurak, Chennupati Jagadish, David Victor Thiel,
Proc. of SPIE Vol. 6415, 641504, (2006) · 0277-786X/06/$15 · doi: 10.1117/12.695611

Downloaded From: https://www.spiedigitallibrary.org/conference-proceedings-of-spie on 4/26/2018 Terms of Use: https://www.spiedigitallibrary.org/terms-of-use

In view of the importance of silicon as the primary semiconductor material in modern microelectronic devices, efforts to control its electronic properties and to tailor the chemical and physical characteristics of its surface are of major importance. We have previously reported the preparation of well-aligned carbon nanotube arrays on silicon (100) surfaces by reaction of a hydride-terminated silicon (100) with ethyl undecylenate to give self-assembled monolayers that were linked by stable silicon-carbon covalent bonds [7]. The ester terminus of the monolayer was subsequently converted to an alcohol whereupon shortened carbon nanotubes were covalently attached using carbodiimide coupling. However, the presence of the self-assembled monolayer of organic material hindered electron transport between carbon nanotubes and the underlying silicon substrate. In addition, the deformation and distortion of the self-assembled molecules will give rise to non-alignment of carbon nanotube layer.

Thus methods to covalently attach carbon nanotubes to silicon without the use of intermediate molecules are of great interest. Hydroxyl terminated silicon is a potential substrate for this purpose. The properties of hydroxyl terminated silicon are well known [8, 9] and a standard procedure has already been established for its preparation [10, 11]. The purpose of this paper is to demonstrate for the first time the attachment of shortened carbon nanotubes to a silicon (100) substrate by direct chemical anchoring to produce a vertically aligned architecture. This is achieved by a condensation reaction between surface hydroxyl groups and carboxylic acid groups on the carbon nanotube. The preparation of the SWCNTs directly attached to a silicon surface was characterised using X-ray photoelectron (XPS), Raman spectroscopies, Atomic Force Microscopy (AFM) and their resultant optical properties can be studied unambiguously.

2. EXPERIMENTAL

2.1 Preparation of SWCNTs directly attached to silicon (100)

Highly boron doped p-type silicon (100) wafers (0.5 mm thickness, 1 mΩ.cm resistivity and polished on one side) were purchased from Virginia Semiconductor, Inc. USA. The surfaces ($0.5\times0.5cm^2$ size) were ultrasonically cleaned in acetone (99.5%, Merck) for 30 seconds and flushed with copious amounts of Milli Q water (18 MΩ.cm). Subsequently the silicon pieces were immersed first in a 1:1:5 mixture of 30% NH_4OH (Sigma-Aldrich), 30% H_2O_2 (Sigma-Aldrich) and Milli Q water (18 MΩ.cm) for 15 minutes at 80 ^oC, followed by immersion in a 1:1:5 mixture of 36% HCl (Ajax Finechem), 30% H_2O_2 (Sigma-Aldrich) and Milli Q water (18 MΩ.cm) for 15 minutes at 80 ^oC [10]. The hydroxyl terminated silicon was incubated in a DMSO (99.9%, ACS Spectrophotometric Grade, Sigma-Aldrich) solution containing both 0.1mg mL^{-1} dicyclohexyl carbodiimide (DCC, 99%, Aldrich) and 0.12mg mL^{-1} functionalised carbon nanotubes. The nanotubes are RFP-SWCNT from Carbon Solutions, Inc. USA cut for 8 hours in mixed acid as described previously [5, 7] and suspended in DMSO. The silicon substrates are exposed to the nanotube solution for different exposure times to give carbon nanotubes directly attached to silicon surfaces. After exposure, the samples are rinsed in copious amounts of acetone to remove any unbound reagents. Figure 1 shows a schematic representation of the preparation of SWCNTs directly attached to silicon.

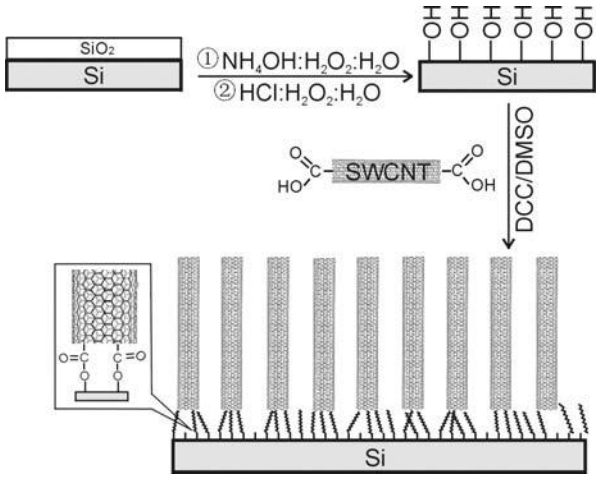

Fig. 1. Schematic representation of the preparation of SWCNTs directly attached to silicon.

Downloaded From: https://www.spiedigitallibrary.org/conference-proceedings-of-spie on 4/26/2018 Terms of Use: https://www.spiedigitallibrary.org/terms-of-use

2.2 X-ray photoelectron spectroscopy (XPS)

X-ray photoelectron spectra were obtained using an Axis Ultra (Kratos Analytical, UK) XPS spectrometer equipped with an Al Kα source (1486.6eV). The take-off angle for detection was nominally 90° from the surface. The pressure in the analysis chamber was less than 5×10^{-8} Torr during analysis. Spectra of the C1s (276-296eV binding energy) regions and survey scans (0-1000eV binding energy) were recorded. The analysis of high-resolution XPS peaks was performed using the Computer Aided Surface Analysis for X-ray Photoelectron Spectroscopy (Casa XPS) software with 30% Lorentzian and 70% Guassian functions and using a Shirley baseline subtraction.

2.3 Raman spectroscopy

A commercial Raman microscope (Renishaw Ramascope System 1000) was used to collect Raman scattered light. The system consists of a single spectrograph fitted with holographic notch filters and a Peltier cooled CCD detector upon which the Raman spectrum is dispersed. The spectrograph is coupled to a Leica microscope (DMLM) with computer controlled sample stage, rigidly fixed to the spectrograph baseplate. The spectrometer has a maximum lateral resolution of 2 μm and depth resolution of 2 mm, however, the effective field of view was increased to allow signal collection from a larger area. The 785 nm laser (Renishaw-badged compact diode laser) was used for the spectra reported in this work, and was focused onto the sample using an x50 objective (Leica, NA = 0.75).

2.4 Atomic Force Microscopy (AFM)

Atomic Force Microscope tapping mode images were taken in air with a multi-mode head and Nanoscope IV controller (Digital Instruments, Veeco, Santa Barbara). Commercially available silicon cantilevers (FESP-ESP series, Veeco probes, Santa Barbara) with fundamental resonance frequency between 70-85 KHz were used. Topographic (height) and amplitude images were obtained simultaneously at a scan rate of 1Hz with the parameters of set point, amplitude, scan size, and feedback control optimised for each sample. All images presented represent background subtracted data using the 'flatten' feature in the Digital Instruments software.

2.5 Fluorescence spectroscopy

A Cary Eclipse Fluorescence spectrometer equipped with solid sample holder accessory was used to investigate the fluorescence properties of carbon nanotube modified silicon surface. Hydroxyl terminated silicon (100) was used as a reference surface. The fluorescence emission spectra were obtained by exciting at 440nm, 473nm and 510 nm respectively with both excitation and emission slit widths set at 20 nm.

3. RESULTS AND DISCUSSION

3.1 X-ray Photoelectron Spectra

Figure 2 shows the X-ray photoelectron survey spectrum for the hydroxyl terminated silicon and the SWCNTs directly attached to silicon. For the hydroxyl terminated silicon (100) surface (curve a in Figure 2), we observe Si2s, Si2p, O1s and Oxygen Auger peaks at binding energies of 99.5eV, 151.5eV, 531.6eV and 979.5eV respectively. After being exposed to the functionalised carbon nanotube suspension for 24 hours, the peak at binding energy 285eV appears, which is due to the presence of carbon. The high resolution C1s spectrum of the SWCNTs directly attached to silicon (shown in Fig 3) is deconvoluted by Casa XPS software into 5 peaks at binding energy 284.6 eV, 286.1 eV, 287.4 eV, 289.1 eV and 290.7 eV. Like the high resolution C1s XPS peak characterization of chemical functionalised SWCNTs [12], the C1s peak has five components and each component has similar peak position. So the following bonds are assigned: 284.6eV (sp^2 C=C / sp^3 C-C), 286.1eV (C-O), 287.4eV (C=O) and 289.1eV (-COO). The peak at 290.7eV is assigned to the π band shake-up satellite for C1s in shortened carbon nanotubes, which involves the energy of $\pi \rightarrow \pi^*$ transition [12, 13]. The peak size of carboxylic groups in this case is relatively higher than that in the literature [12]. This is due to the fact that carbon nanotubes had been functionalised using an oxidising mixture of strong acids before the surface reaction, which introduced plenty of carboxylic groups onto the sidewall and open ends of carbon nanotubes.

Downloaded From: https://www.spiedigitallibrary.org/conference-proceedings-of-spie on 4/26/2018 Terms of Use: https://www.spiedigitallibrary.org/terms-of-use

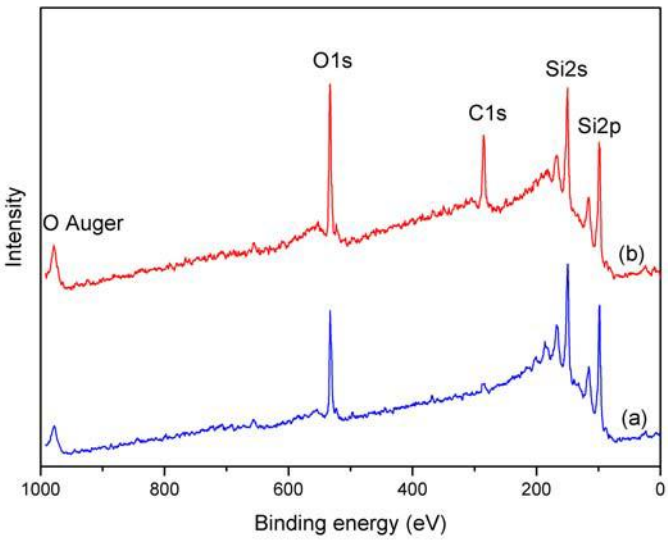

Fig. 2. XPS spectra for the hydroxyl terminated silicon (a) and the SWCNTs directly attached to silicon after 24 hrs exposure at 80 ^{o}C (b).

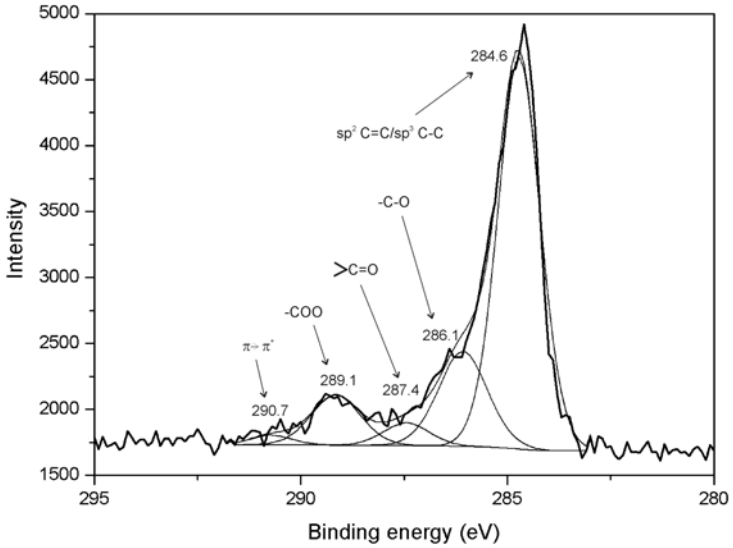

Fig. 3. High resolution C1s XPS spectrum for the SWCNTs directly attached to silicon.

3.2 Raman Spectroscopy

Figure 4 shows typical Raman spectra for the hydroxyl terminated silicon and SWCNTs directly attached to silicon, where the SWCNTs directly attached to silicon was prepared with 24 hours exposure at 80 ^{o}C. For the hydroxyl terminated silicon, we can only observe a broad band at 950 cm^{-1}, which is due to bulk silicon. By comparison to the hydroxyl terminated silicon, the SWCNTs directly attached to silicon spectrum has two resonance-enhanced Raman bands at 1595 cm^{-1} and 1314 cm^{-1}. The difference spectrum is shown as curve (c) in Figure 4. Two peaks appearing on curve (c) are well-known as the tangential band (G band) and the disorder-induced band (D band) for single-walled carbon nanotubes [14, 15]. The G band provides information about the chirality of SWCNTs, where different chiralities yield either semiconducting and metallic nanotubes. The D band on the other hand provides information on the purity of the carbon nanotubes and how ordered the graphene structure of the nanotubes are, as the size of the peak gives an indication of the amount of amorphous and poorly organized material is present in the sample [14, 16]. In Figure 4c, the ratio of D/G is 0.31, which is considerably larger than the values of 0.01 for the isolated as-prepared single-walled

Downloaded From: https://www.spiedigitallibrary.org/conference-proceedings-of-spie on 4/26/2018 Terms of Use: https://www.spiedigitallibrary.org/terms-of-use

carbon normally [14], and 0.1 for the vertically aligned SWNCT arrays prepared by molecular beam-controlled nucleation and growth [17]. The larger D/G value can be attributed to the defects on the sidewall of carbon nanotube caused by cutting process in mixed acids.

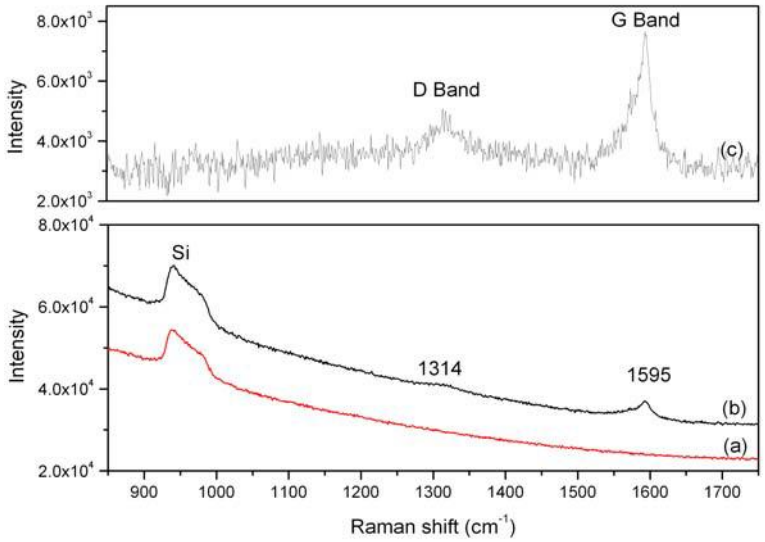

Fig. 4. Typical Raman spectra using a λ=785nm laser line for hydroxyl terminated silicon (a) and SWCNTs directly attached to silicon (b). Curve (c) is the difference spectrum obtained by subtracting Curve (a) from Curve (b).

3.3 Atomic Force Microscopy

Figure 5 shows tapping mode AFM images of silicon substrates exposed to the SWCNTs solution for various exposure times. Before attachment of functionalised carbon nanotubes, the hydroxyl terminated silicon pieces are observed to be very flat surfaces. However, after the surface condensation reaction, protrusions are clearly observed in AFM images (Figures 5a-c). At the short exposure times (e. g. 2 hours, shown in Figure 5.a), well-separated carbon nanotube islands can be seen with large areas of bare silicon surface between. As the exposure time increases, both the number and size of carbon nanotube islands increase. The coverage for different exposure times has been measured to be 36% after 2h exposure; 85% after 20h exposure and 90% after 100h exposure. The average island diameters are ~95nm for 2h exposure, ~110nm for 20h exposure, and ~140nm for 100h exposure. The observed increase in diameter as a function of exposure time is consistent with the formation of nanotube bundles. The average (and maximum) height was also measured via AFM, and found to be 22.9nm (41.1nm) after 2h exposure; 29.8nm (72.0nm) after 20h exposure; and 35.5nm (101.5 nm) after 100h. Again, the trend shows an increasing height with reaction time, as one would expect. The separated SWCNTs islands shown in Figure 5a support an island growth model.

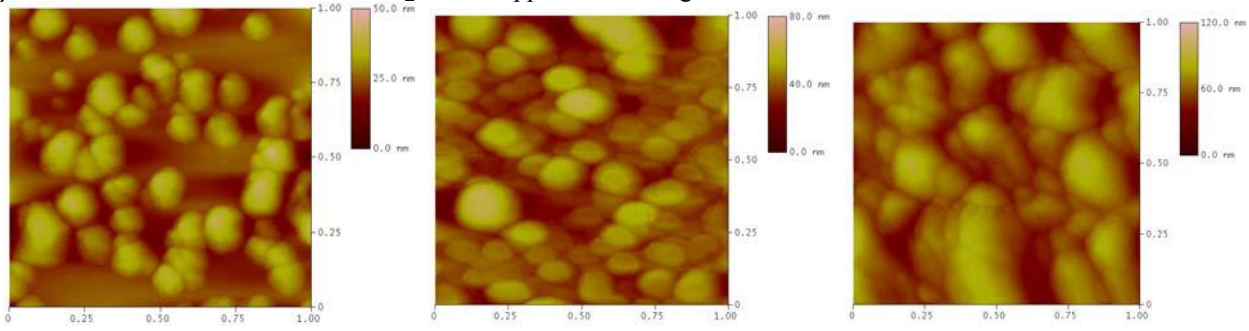

(a) (b) (c)

Fig. 5. Tapping mode AFM images for the SWCNTs directly attached to silicon surfaces for different exposure times at 80°C, where (a) 2 hours, (b) 20 hours and (c) 100 hours exposure time with scan size 1μm×1μm.

Downloaded From: https://www.spiedigitallibrary.org/conference-proceedings-of-spie on 4/26/2018 Terms of Use: https://www.spiedigitallibrary.org/terms-of-use

3.4 Fluorescence spectroscopy

Following excitation at various wavelengths between 440 nm and 510 nm, SWCNTs directly attached to a silicon surface exhibit strong fluorescence in the wavelength range from 650-800 nm. The excitation spectrum for this nanostructure shows peaks at 442 nm, 473 nm, 513 nm, 563 nm and 594 nm. Exciting the system at different wavelengths yields fluorescence shifted well to the red of the excitation wavelength. Figure 6 shows the fluorescence emission spectra for SWCNT directly modified on silicon when using different excitation wavelengths.

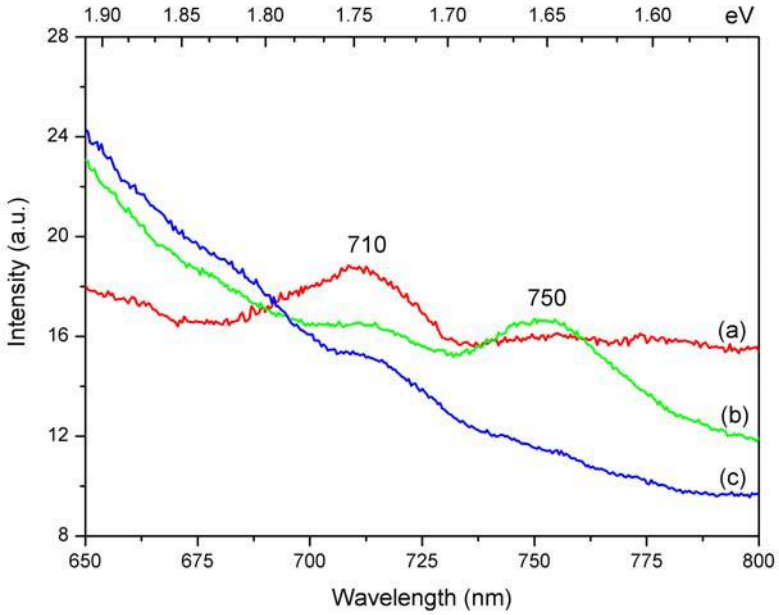

Fig. 6. Fluorescence emission spectra for SWCNT directly modified silicon when the surface was excited by different wavelengths, (a) 440nm, (b) 473nm and (c) 510nm.

It is very apparent that the emission spectra show strong excitation wavelength dependence. In detail, when the surface was excited at 440 nm, only one emission peak at 710nm (1.75eV) was observed. However, when the surface was excited at 473nm, a new emission peak at 750nm (1.66eV) is observed while the existing emission peak at 710nm is reduced in intensity. Interestingly when the surface was excited at 510nm, the emission peak at 750 nm disappears altogether and while the peak at 710nm remains, it is quite small. The fluorescence linewidths of 710nm(λ_{ex}=440 nm) and 750nm(λ_{ex}=473 nm) are 26.1 nm (0.065eV) and 23.4 nm (0.052eV) respectively. No fluorescence is observed for unattached nanotubes while a small, continuous background fluorescence is observed for the bare hydroxyled substrate. The bare substrate is used as the reference in these experiments so the fluorescence observed for the nanostructure is over and above this.

To our knowledge, no similar observations of fluorescence emission have been reported for a SWCNTs/silicon structure even though there are several examples of vertically-aligned SWCNT arrays. Both emission peaks cannot be simply assigned to the silicon substrate, because bulk crystalline silicon has a band gap of 1.1 eV and should result in luminescence in the near infrared region (~1100nm). Additionally, the band gap fluorescence from individual semiconducting SWCNTs has been theoretically predicted and experimentally confirmed in the 800-1600 nm region of the near infrared[18, 19]. However a further complicating issue is that the photoluminescence intensity is dramatically reduced by aggregation of isolated nanotubes [18-20]. In these experiments, the fact that SWCNTs bundle together even after 2 hours exposure has been shown using AFM and SEM. Moreover the linewidths of emission spectra should be approximately 10 nm (0.025eV) if the fluorescence is from individual SWCNTs [18, 19]. Both of the peak linewidths for SWCNTs directly attached to silicon are greater than this value, indicating that the attached SWCNTs exhibit a different mechanism than individual SWCNT. In this case the fluorescence must be attributable a combined effect involving the attached SWCNTs and silicon substrate.

Downloaded From: https://www.spiedigitallibrary.org/conference-proceedings-of-spie on 4/26/2018 Terms of Use: https://www.spiedigitallibrary.org/terms-of-use

The lack of emission from the separate components means that the observed fluorescence must be due to something in the newly created nanostructure. One possibility is the newly formed ester linkage. This seems unlikely as the observed shifts in fluorescence wavelengths for esters typically used in flow cytometry experiments is tens of nanometers [21]. Additionally, if the ester linkage did fluoresce one might expect some fluorescence from the carboxylic acid group of the cut nanotubes before surface attachment and this is not observed.

The large shift between the excitation wavelengths and the observed emission suggest that one species may be excited while a second is fluorescing. Indeed, there are a few cases of large shifts in the fluorochromes commercially available but these all involve conjugates of two quite different species [22]—one for excitation and one for emission. In the case the silicon nanostructure formed in this work, it is thought that the nanotubes are excited but then strongly couple to the electronic states of the substrate, allowing an intersystem crossing of energy into the silicon band structure. Emission from porous silicon is well established since Canhan and others [23, 24] discovered that electrochemically etched porous silicon possessed remarkable optical properties. While emission from porous silicon can be observed over a wide range of wavelengths, the S band has peak intensity in the region where the emission in this work is observed [25]. Additionally, recent work has shown porous silicon emission spectra with peak intensities in the 650 nm region obtained using excitation between 400 and 450 nm [26]. The nanostructure here physically resembles porous silicon to some extent as shown in Figure 5. Observation of dramatically shifted fluorescence emission indicates a very strong coupling of the electronic states of the nanotubes and the substrate. In essence, the two components of the nanostructure seem to be coupled electronically to such an extent to appear much like one integrated structure.

4. CONCLUSIONS

This work successfully demonstrates a new approach for the fabrication of vertically-aligned shortened carbon nanotube architectures on a silicon (100) substrate by direct chemical anchoring. Compared to other techniques, this new technique has several advantages including the low temperature involved and the possibility for further modification. The attachment of the SWCNTs directly to the silicon surface provides a simple and new avenue for the fabrication and development of silicon-based sensors, solar cells and nanoelectronic devices using further surface modification.

REFERENCES

1. Zhu, L.B., Sun, Y.Y., Hess, D.W., and Wong, C.P. (2006). Well-aligned open-ended carbon nanotube architectures: An approach for device assembly. Nano Letters *6*, 243-247.
2. Liu, Z.F., Shen, Z.Y., Zhu, T., Hou, S.F., Ying, L.Z., Shi, Z.J., and Gu, Z.N. (2000). Organizing single-walled carbon nanotubes on gold using a wet chemical self-assembling technique. Langmuir *16*, 3569-3573.
3. Ren, Z.F., Huang, Z.P., Xu, J.W., Wang, J.H., Bush, P., Siegal, M.P., and Provencio, P.N. (1998). Synthesis of large arrays of well-aligned carbon nanotubes on glass. Science *282*, 1105-1107.
4. Fan, S.S., Chapline, M.G., Franklin, N.R., Tombler, T.W., Cassell, A.M., and Dai, H.J. (1999). Self-oriented regular arrays of carbon nanotubes and their field emission properties. Science *283*, 512-514.
5. Gooding, J.J., Wibowo, R., Liu, J.Q., Yang, W.R., Losic, D., Orbons, S., Mearns, F.J., Shapter, J.G., and Hibbert, D.B. (2003). Protein electrochemistry using aligned carbon nanotube arrays. Journal of the American Chemical Society *125*, 9006-9007.
6. Jung, D.H., Kim, B.H., Ko, Y.K., Jung, M.S., Jung, S., Lee, S.Y., and Jung, H.T. (2004). Covalent attachment and hybridization of DNA oligonucleotides on patterned single-walled carbon nanotube films. Langmuir *20*, 8886-8891.
7. Yu, J., Losic, D., Marshall, M., Böcking, T., Gooding, J.J., and Shapter, J.G. (2006). Preparation and characterisation of an aligned carbon nanotube array on silicon (100) surface. Submitted to Soft Matter.
8. Buriak, J.M. (2002). Organometallic chemistry on silicon and germanium surfaces. Chemical Reviews *102*, 1271-1308.
9. Cerofolini, G.F., Arena, G., Camalleri, C.M., Galati, C., Reina, S., Renna, L., and D., M. (2005). A hybrid approach to nanoelectronics. Nanotechnology *16*, 1040–1047.
10. Wu, X.C., Bittner, A.M., and Kern, K. (2004). Microcontact printing of CdS/dendrimer nanocomposite patterns on silicon wafers. Advanced Materials *16*, 413-+.
11. Wu, X.C., Bittner, A.M., and Kern, K. (2002). Spatially selective electroless deposition of cobalt on oxide surfaces directed by microcontact printing of dendrimers. Langmuir *18*, 4984-4988.

Downloaded From: https://www.spiedigitallibrary.org/conference-proceedings-of-spie on 4/26/2018 Terms of Use: https://www.spiedigitallibrary.org/terms-of-use

12. Okpalugo, T.I.T., Papakonstantinou, P., Murphy, H., McLaughlin, J., and Brown, N.M.D. (2005). High resolution XPS characterization of chemical functionalised MWCNTs and SWCNTs. Carbon *43*, 153-161.
13. Moulder, J.F., Stickle, W.F., Sobol, P.E., and Bomben, K.D. (1992). Handbook of X-ray Photoelectron Spectroscopy (Physical Electronics Division, Perkin-Elmer Corporation, USA).
14. Jorio, A., Pimenta, M.A., Souza, A.G., Saito, R., Dresselhaus, G., and Dresselhaus, M.S. (2003). Characterizing carbon nanotube samples with resonance Raman scattering. New Journal of Physics *5*, 139.131-139.117.
15. Pimenta, M.A., Marucci, A., Empedocles, S.A., Bawendi, M.G., Hanlon, E.B., Rao, A.M., Eklund, P.C., Smalley, R.E., Dresselhaus, G., and Dresselhaus, M.S. (1998). Raman modes of metallic carbon nanotubes. Physical Review B *58*, 16016-16019.
16. Anglaret, E., Bendiab, N., Guillard, T., Journet, C., Flamant, G., Laplaze, D., Bernier, P., and Sauvajol, J.L. (1998). Raman characterization of single wall carbon nanotubes prepared by the solar energy route. Carbon *36*, 1815-1820.
17. Eres, G., Kinkhabwala, A.A., Cui, H.T., Geohegan, D.B., Puretzky, A.A., and Lowndes, D.H. (2005). Molecular beam-controlled nucleation and growth of vertically aligned single-wall carbon nanotube arrays. Journal of Physical Chemistry B *109*, 16684-16694.
18. O'Connell, M.J., Bachilo, S.M., Huffman, C.B., Moore, V.C., Strano, M.S., Haroz, E.H., Rialon, K.L., Boul, P.J., Noon, W.H., Kittrell, C., Ma, J.P., Hauge, R.H., Weisman, R.B., and Smalley, R.E. (2002). Band gap fluorescence from individual single-walled carbon nanotubes. Science *297*, 593-596.
19. Hartschuh, A., Pedrosa, H.N., Novotny, L., and Krauss, T.D. (2003). Simultaneous fluorescence and Raman scattering from single carbon nanotubes. Science *301*, 1354-1356.
20. Ago, H., Imamura, S., Okazaki, T., Saitoj, T., Yumura, M., and Tsuji, M. (2005). CVD growth of single-walled carbon nanotubes with narrow diameter distribution over Fe/MgO catalyst and their fluorescence spectroscopy. Journal Of Physical Chemistry B *109*, 10035-10041.
21. Berlier, J.E., Rothe, A., Buller, G., Bradford, J., Gray, D.R., Filanoski, B.J., Telford, W.G., Yue, S., Liu, J.X., Cheung, C.Y., Chang, W., Hirsch, J.D., Beechem, J.M., Haugland, R.P., and Haugland, R.P. (2003). Quantitative comparison of long-wavelength Alexa Fluor dyes to Cy dyes: Fluorescence of the dyes and their bioconjugates. Journal of Histochemistry & Cytochemistry *51*, 1699-1712.
22. Roederer, M., Kantor, A.B., Parks, D.R., and Herzenberg, L.A. (1996). Cy7PE and Cy7APC: Bright new probes for immunofluorescence. Cytometry *24*, 191-197.
23. Canham, L.T. (1990). Silicon quantum wire array fabrication by electrochemical and chemical dissolution of wafers. Applied Physics Letters *57*, 1046-1048.
24. Rowsell, B.D., and Veinot, J.G.C. (2005). Reductive thermolysis of a heterocyclic precursor: a convenient method for preparing luminescent, surfactant-stabilized silicon nanoparticles. Nanotechnology *16*, 732-736.
25. Cullis, A.G., Canham, L.T., and Calcott, P.D.J. (1997). The structural and luminescence properties of porous silicon. Journal of Applied Physics *82*, 909-965.
26. Moyer, P.J., Pridmore, A., Martin, T., Schmidt, J., Hasche, T., Eng, L., and Gole, J.L. (2000). Dependence of radiative lifetimes of porous silicon on excitation wavelength and intensity. Applied Physics Letters *76*, 2683-2685.

Downloaded From: https://www.spiedigitallibrary.org/conference-proceedings-of-spie on 4/26/2018 Terms of Use: https://www.spiedigitallibrary.org/terms-of-use